Archives of Biochemistry and Biophysics 610 (2016) 8–15

Contents lists available at ScienceDirect

Archives of Biochemistry and Biophysics

journal homepage: www.elsevier.com/locate/yabbi

Olfactory signaling components and olfactory receptors are expressed in tubule cells of the human kidney

Benjamin Kalbe [a, *], Marian Schlimm [a], Sebastian Wojcik [a], Stathis Philippou [b], Désirée Maßberg [a], Fabian Jansen [a], Paul Scholz [a], Hermann Luebbert [c], Burkhard Ubrig [d], Sabrina Osterloh [a], Hanns Hatt [a]

[a] Department of Cell Physiology, Ruhr-University Bochum, Bochum, Germany
[b] Department of Pathology and Cytology, Augusta-Kranken-Anstalt, Bochum, Germany
[c] Department of Animal Physiology, Ruhr-University Bochum, Bochum, Germany
[d] Clinic for Urology, Augusta-Kranken-Anstalt, Bochum, Germany

ARTICLE INFO

Article history:
Received 12 August 2016
Received in revised form
26 September 2016
Accepted 28 September 2016
Available online 28 September 2016

Keywords:
Olfactory receptors
GPCR
Proximal tubule
Signaling
Calcium
Physiology

ABSTRACT

Cells of the renal tubule system are in direct contact with compounds dissolved in the urine, such as short chain fatty acids (SCFA). Murine OR78, a member of the olfactory receptor (OR) family, is involved in SCFA-related regulation of renal blood pressure in mice. It is still unclear whether OR signaling has an impact on human renal physiology. In our study, we showed that OR51E1 and OR11H7, both of which can be activated by the SCFA isovaleric acid, are expressed in the HK-2 human proximal tubule cell line. We observed a transient increase in intracellular Ca^{2+} when isovaleric acid and 4-methylvaleric acid were added to HK-2 cells. The isovaleric acid-induced response was dependent on extracellular Ca^{2+} and adenylyl cyclase (AC) activation. Furthermore, we demonstrated that the canonical olfactory signaling components $G\alpha_{olf}$ and ACIII are co-localized with OR51E1. The number of cells responding to isovaleric acid correlated with the presence of primary cilia on HK-2 cells. OR51E1 protein expression was confirmed in the tubule system of human kidney tissue. Our study is the first to show the expression of ORs and olfactory signaling components in human kidney cells. Additionally, we discuss ORs as potential modulators of the renal physiology.

1. Introduction

Olfactory receptors (ORs) are G protein-coupled receptors (GPCRs) that form the largest known gene superfamily in the human genome. Their expression was first described in the olfactory epithelium (OE) [1]. However, current studies have also verified the functional expression of ORs in non-olfactory human tissues, where they play essential roles in physiological processes. For example, ORs impact sperm motility [2], inhibition of proliferation of prostate and liver cancer cells, as well as myelogenous leukemia cells [3–5], wound healing of human skin [6], and serotonin release of enterochromaffin cells [7]. Therefore, ORs seem to have diverse physiological and pathophysiological functions and are interesting targets for basic and clinical research approaches. In olfactory sensory neurons, the binding of an odorant to an OR leads to the activation of a cAMP-mediated signaling pathway. The olfactory specific G protein $G\alpha_{olf}$ is activated after the conformational change of the receptor and in turn activates adenylyl cyclase III (ACIII), which converts ATP to cAMP [8–10]. The production of cAMP leads to the opening of cyclic nucleotide-gated (CNG) channels and an influx of Ca^{2+} into the sensory neuron [11,12]. Interestingly, a previous study revealed the expression of olfactory signaling components $G\alpha_{olf}$ and ACIII in cells of the macula densa of rat and mice kidney [13]. ACIII-deficient mice showed a reduced glomerular filtration rate (GFR), and it is assumed that both $G\alpha_{olf}$ and ACIII play a role in the regulation of the GFR and blood pressure [14]. Further, OR78, a short chain fatty acid (SCFA)-activated receptor, is expressed in cells of the macula densa and has an impact on the modulation of blood pressure and renin secretion in the mouse kidney. ORs are therefore good candidates for the detection of fatty acids dissolved within the filtrate of the kidney glomeruli. The production of SCFA is associated with the fermentation of gut

* Corresponding author. Department of Cell Physiology, Ruhr-University Bochum, ND 4/169, Universitaetsstr. 150, D-44780 Bochum, Germany.
E-mail address: benjamin.kalbe@rub.de (B. Kalbe).

http://dx.doi.org/10.1016/j.abb.2016.09.017
0003-9861/

microbiota, but the accumulation of SCFA can also occur during pathological processes and change the odor of the urine. Patients with isovaleric aciduria, a genetic disorder of the leucine metabolism, exhibit an increased accumulation of isovaleric acid (IVA) that gives urine the odor of sweaty feet [15].

Until now, no studies have documented expression of ORs in cells of the human kidney. In this study, we demonstrated that some components of the olfactory signaling cascade and OR51E1 and OR11H7 are expressed in the human proximal tubule cell line HK-2. We showed that HK-2 cells can be activated by IVA, a ligand for OR51E1 and OR11H7. These findings could be useful for understanding the modulation of renal physiology by SCFA-sensing GPCRs.

2. Materials and methods

2.1. Cultivation of HK-2 cells

HK-2 cells were the kind gift of Dr. Ulla Ludwig (Department of Internal Medicine I, University of Ulm, Ulm, Germany). HK-2 cells were cultured in DMEM/F12 supplemented with 10% fetal bovine serum (FBS) and 100 U/ml of penicillin and streptomycin at 37 °C in a 5% CO_2 humidified atmosphere. Gibco™ supplements and media were purchased from Thermo Fisher Scientific (Waltham, USA) unless indicated otherwise.

2.2. Total RNA isolation and reverse transcriptase (RT)-PCR

Total RNA was extracted from HK-2 cells using an RNeasy® Mini Kit (Qiagen, Germany) according to the manufacturer's instructions. RNA concentration and quality (A260/A280 ratio) were analyzed using a NanoDrop ND-1000 Spectrophotometer (Thermo Scientific, USA). After DNase I treatment with a TURBO DNA-free™ Kit (Thermo Scientific, USA), complementary DNA (cDNA) was synthesized using an iScript™ cDNA Synthesis Kit (Bio-Rad, Berkeley, USA). For RT-PCR experiments, we used RNA controls (−RT) to exclude genomic DNA contamination. RT-PCR was performed using the GoTaq® qPCR Master Mix (Promega, USA) in a volume of 20 µl with 10 pmol of each primer. The following temperature cycle profile was used: 5 min at 95 °C followed by 40 cycles of 45 s at 95 °C, 45 s at 60 °C, 45 s at 72 °C and a final extension of 10 min at 72 °C. The following primers were used: β-actin (forward: 5′-GTACCCAGGCATTGCTGACA-3′, reverse: 5′-AGAAAGGGTGTAAAACGCAGC-3′), OR51E1 (forward: 5′-TTTGGCACTTGCGTCTCTCA-3′, reverse: 5′-GACACCTAGGGCTCTGAAGC-3′), OR11H7 (forward: 5′-TCCTCTGCCCCTACTCACAT-3′, reverse: 5′-GGCTGTAGATGAGGGGGTTT-3′), GNAL (forward: 5′-CAGACCAGGACCTCCTCAGA-3′, reverse: 5′-AGGGACTCTCTCAGCCTGTT-3′), and ADCY3 (forward: 5′-AAGGATTCAACCCTGGGCTC-3′, reverse: 5′-TCCAGCGTCGCATCTCATAG-3′).

2.3. Protein extraction and western blotting

Kidney tissues were obtained from patients undergoing surgical operations. Tissue collection was conducted according to the Declaration of Helsinki, and all patients gave their written consent. Whole protein lysate was extracted after sedimentation of cells or tissue in an appropriate volume of radioimmunoprecipitation assay (RIPA) buffer with protease inhibitors, followed by mechanical homogenization and a final centrifugation (1000 g for 10 min at 4 °C). For phosphorylation analysis, PhoshStop was added to RIPA buffer. A sample of the whole protein fraction was collected and prepared in Laemmli's buffer for Western blot analysis. For the membrane preparation, whole protein lysate was subjected to ultracentrifugation (35,000 g for 2 h). The precipitate and a sample of the supernatant were dissolved in Laemmli's buffer for further western blot analyses. Western blots were performed as described elsewhere (Neuhaus et al., 2009). After SDS-PAGE, proteins were transferred onto nitrocellulose membranes in a blotting chamber with 100 V at 4 °C for 30 min. After blocking at room temperature for 1 h in 50% casein (50% TBS buffer and 50% casein in TBS), membranes were incubated with primary antibodies against OR51E1 (custom designed, polyclonal, Eurogentec, Belgium) (Flegel et al., 2016), ACIII (Santa Cruz Biotechnology, USA), and $G\alpha_{olf}$ (Santa Cruz Biotechnology, USA) in a 1:250 dilution in 75% TBS buffer and 25% casein at 4 °C overnight. Nitrocellulose membranes were washed with TBS-T (3X, 10 min). For immunodetection, membranes were incubated with horseradish peroxidase (HRP)-coupled secondary antibodies (goat anti-rabbit, rabbit anti-goat, Bio-Rad, UK) diluted 1:10,000 in 75% TBS buffer with 25% casein at room temperature for 45 min. After additional TBS-T washes (3X, 10 min), chemiluminescence was imaged via Fusion-SL 3500-WL (Vilber Lourmat).

2.4. Immunocytochemical staining of HK-2 cells

HK-2 cells were cultured on 30 mm coverslips until 80% confluent. After washing in PBS, cells were fixed in ice-cold acetone for 5 min. To avoid nonspecific antibody binding, cells were blocked in 1% cold water fish gelatin (Sigma-Aldrich, USA) diluted in TBS with 0.05% Triton X-100 (Sigma-Aldrich, USA) before incubating with primary antibodies against OR51E1, ACIII, and $G\alpha_{olf}$ (dilution: 1:50). Cells were co-incubated with DAPI fluorescent dye to label the nucleus and washed 3 times in PBS for 10 min. Fluorophore-coupled secondary antibodies (Alexa Fluor 488 nm or 546 nm, Thermo Fisher Scientific, USA) were diluted 1:1000 in 1% fish gelatin/0.05% Triton X-100. After three PBS washes of 10 min each, cells were coated with Prolong Antifade Gold (Life Technologies, USA). Fluorescent signals were detected using a confocal microscope (Zeiss LSM 510 Meta, Germany) with a 40× oil immersion objective. The images were processed with the same settings using Corel Draw X5 (Corel, USA).

2.5. Immunohistochemical staining of kidney tissue

Paraffin-embedded human tissue was deparaffinized using Roti®-Histol (Roth, Karlsruhe, Germany) and dehydrated with isopropanol. The tissue was rehydrated with an ethanol-series and washed twice with 0.01 M PBS. Next, antigen retrieval and permeabilization were performed. To prevent nonspecific primary antibody binding, sections were blocked in 5% normal serum for 10 min. Sections were incubated with anti-OR51E1 antibodies (1:50 dilution) in 0.01 M PBS at 4 °C overnight. Sections were washed again with 0.01 M PBS and incubated with biotinylated secondary antibody (anti-rabbit) for 45 min (1:1000 dilution). A VECTASTAIN®Elite avidin/biotin (ABC)-based Kit (Vector laboratories, Burlingame, USA) was used according to the manufacturer's recommendations. Sections were incubated with 3,3'-diaminobenzidine until sufficiently stained, and the reaction was stopped with 0.1 M PBS at 4 °C. Immunohistochemical staining was detected with an Olympus BX 43 microscope (10× objective).

2.6. Calcium imaging

HK-2 cells cultured in 35-mm cell culture dishes (Sarstedt, Germany) were incubated with 3 µM fura-2-acetoxymethyl ester (Molecular Probes, Thermo Fisher Scientific, USA) for 30 min at 37 °C. The growth medium was exchanged with an extracellular solution and fluorometric imaging was performed as previously described [4]. Depending on the experimental approach, cells were

exposed to odorants using a specialized microcapillary application system. All of the substances were first diluted in DMSO (maximal final concentration of 0.1%) and dissolved in extracellular solution to the desired concentration. Cells were pre-incubated with SQ22536 (200 μM) (Enzo Life Sciences, USA). Data from the calcium imaging experiments were processed using the Leica Application Software (LAS, Germany), and the amplitudes were calculated using Sigma Plot (Systat, USA).

2.7. Odorants and odorant mixtures

The odorant mixture contained three odorants (each at 300 μM) that are known ligands for deorphanized ORs: isovaleric acid, 4-methylvaleric acid, and hexanoic acid. All of the odorants were kindly provided by Dr. J. Panten (Symrise AG, Holzminden, Germany) and were initially dissolved in DMSO.

2.8. Statistical analysis

All results were tested for normality and equal variance. Data that passed the equal variance and normality tests were subjected to a two-tailed unpaired *t*-test. Data that failed the aforementioned tests were subjected to a Mann-Whitney *U* test. All values represent the mean ± standard error of the mean (SEM) of at least three independent experiments. In all figures, the significance of differences is represented as follows: $^{*}p < 0.05$, $^{**}p < 0.01$ and $^{***}p < 0.001$.

3. Results

3.1. 4-Methylvaleric acid and isovaleric acid elicit an increase in cytosolic Ca^{2+} in HK-2 cells

To identify functionally expressed ORs activated by fatty acids in HK-2 cells, we first applied an odorant mixture (OM) containing hexanoic acid (300 μM), 4-methylvaleric acid (4-MVA) (300 μM), and isovaleric acid (IVA) (300 μM). These odorants are known agonists of the following human ORs: OR51L1 (hexanoic acid), OR51E1 (4-MVA), and OR11H4, OR11H6, OR11H7, and OR51E1 (all IVA) [17–20]. Ca^{2+}-imaging measurements showed an increase in the intracellular Ca^{2+} concentration of HK-2 cells after application of the odorant mixture (Fig. 1A). By analyzing odorants singly, we demonstrated that only 4-MVA (300 μM) and IVA (300 μM) elicited a robust transient increase in cytosolic Ca^{2+} (Fig. 1B and C). Furthermore, we observed that IVA induced a Ca^{2+} increase in just a subset of cells (10.241% ± 1.3856%, Fig. 4D) rather than all cells in the field of view (Fig. 1D). To demonstrate cell viability, we added ATP (100 μM) at the end of all experiments. We quantified the amplitudes of the Ca^{2+} responses and observed that, on average, IVA (300 μM) led to higher Ca^{2+} increases (amplitude: 0.2367 ± 0.0711) compared to 4-MVA (300 μM) (amplitude: 0.1421 ± 0.0623) (Fig. 1E). Next, we treated HK-2 cells with increasing concentrations of IVA (30 μM, 300 μM, 1 mM) and observed a concentration-dependent increase in intracellular Ca^{2+} concentration (Fig. 1F).

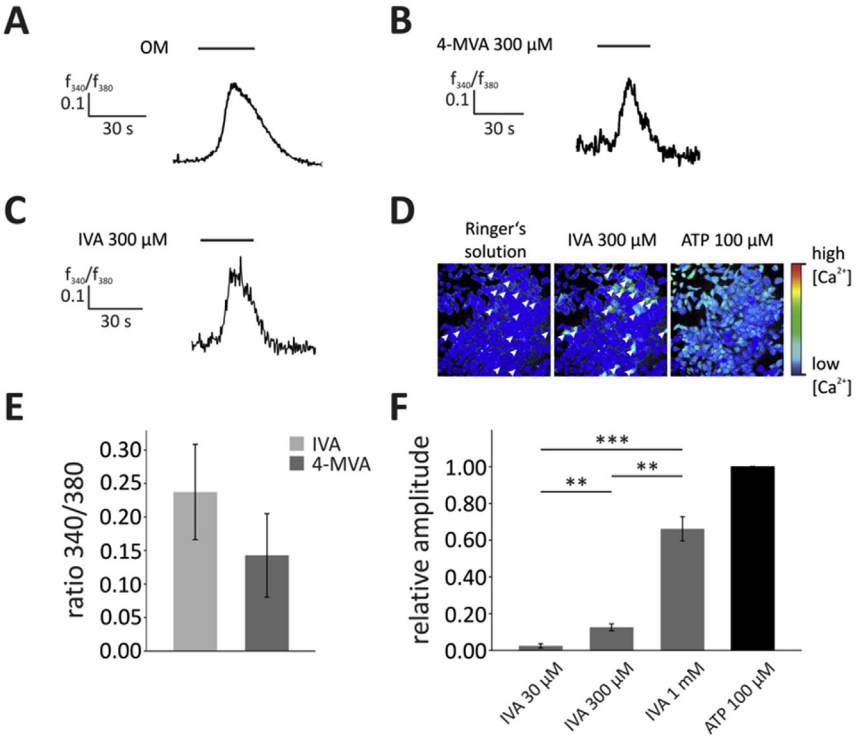

Fig. 1. 4-methylvaleric acid (4-MVA) and isovaleric acid (IVA) elicited an intracellular Ca^{2+} increase in HK-2 cells as measured through ratiofluorometric Ca^{2+} imaging. (A) An odorant mixture (OM) containing hexanoic acid (300 μM), 4-MVA (300 μM), and IVA (300 μM) was applied for 30 s to HK-2 cells, and a transient increase in intracellular Ca^{2+} was observed. (B) The odorant 4-MVA (300 μM) (agonist for OR51E1) was applied to HK-2 cells for 30 s, and a transient rise in intracellular Ca^{2+} concentration was visible. (C) IVA (300 μM) (agonist for OR11H4, OR11H6, OR11H7, and OR51E1) was applied for 30 s to HK-2 cells and induced a transient increase in the intracellular Ca^{2+}. (D) Representative Ca^{2+} imaging recording of Fura-2-loaded HK-2 cells. The changes in the intracellular Ca^{2+} concentration after application of IVA (300 μM) are presented in pseudocolors. The intracellular Ca^{2+} concentration of HK-2 cells before application of IVA (Ringer's solution) and after application of ATP positive control (100 μM) are shown. (E) The amplitudes of cytosolic Ca^{2+} increased after application of 4-MVA (300 μM) (dark gray) (N = 3) and IVA (300 μM) (light gray) (N = 4). (F) Application of IVA in three different concentrations (30 μM, 300 μM, and 1 mM) (N = 6) led to a concentration dependent rise of the amplitude measured in Ca^{2+} imaging experiments. Amplitudes were normalized to ATP (100 μM) positive stimulus. Black bars of all experiments indicate the stimulus duration. All error bars represent the ±SEM of three to six independent experiments. Significance was tested using an unpaired two-sample Student's *t*-test. $^{**}p < 0.01$; $^{***}p < 0.001$.

3.2. OR51E1 and the olfactory signaling components ACIII and $G\alpha_{olf}$ are expressed at the transcript and protein levels

To demonstrate the expression of ORs known to be activated by either 4-MVA or IVA, quantitative PCR experiments with OR-specific primers were performed. OR51E1 and OR11H7 were detected at the transcript level (Fig. 2A). OR11H4 and OR11H6 expression could not be validated (data not shown). After quantification, we found that OR51E1 transcript abundance was significantly higher (ΔCt value: -1.351 ± 0.5708) than that of OR11H7 (ΔCt value: 3.7933 ± 0.1889) (Fig. 2B). In qualitative PCR experiments, we identified GNAL transcripts, which code for the olfactory-specific G protein $G\alpha_{olf}$, and ADCY3 transcripts, which code for adenylyl cyclase III (ACIII) (Fig. 2C). Further, we validated the presence of

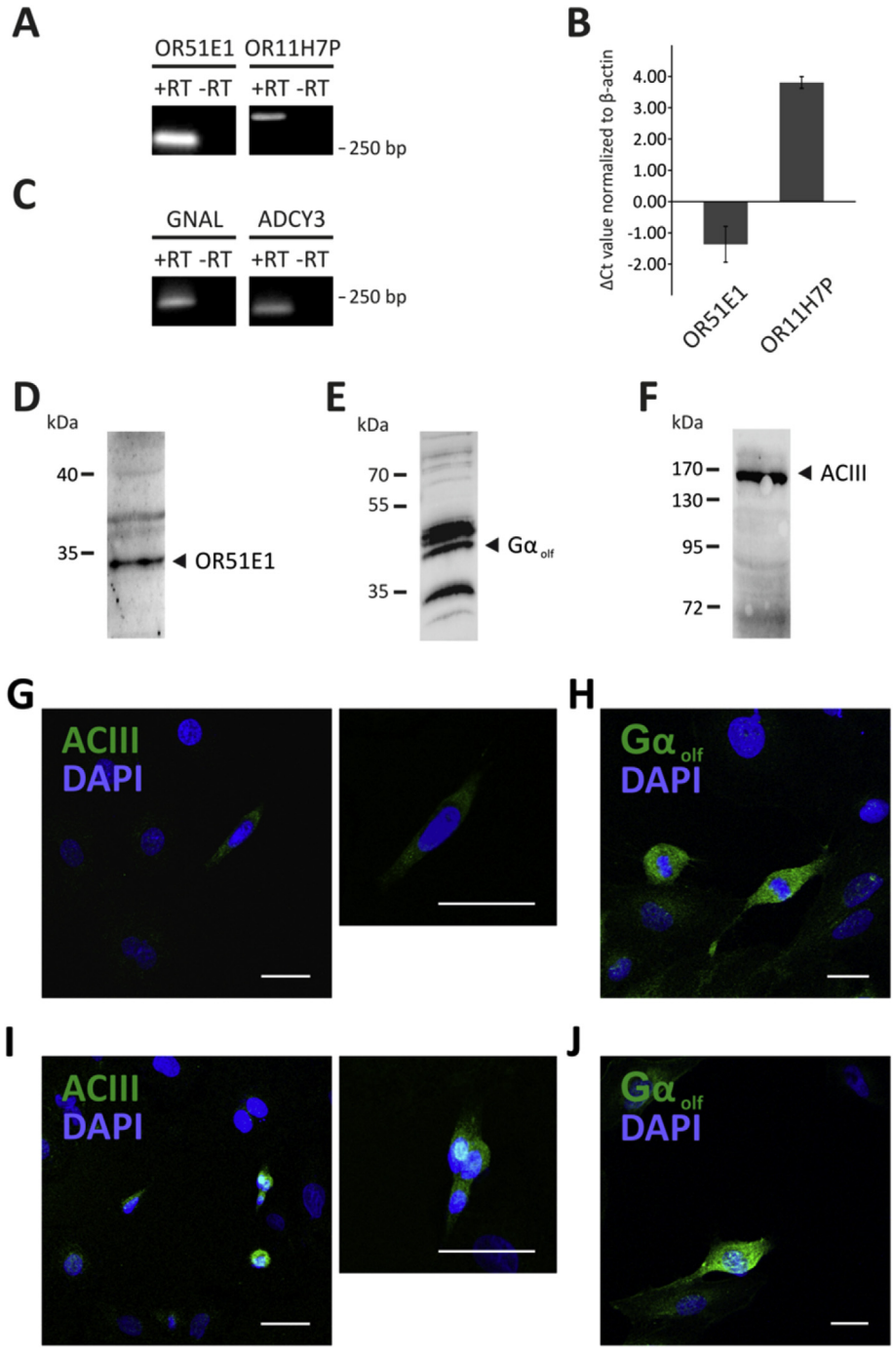

Fig. 2. Olfactory receptor OR51E1 and olfactory signaling components $G\alpha_{olf}$ (GNAL) and ACIII were expressed at the transcript and protein levels in HK-2 cells. (A, B) Transcript abundance of OR51E1 and OR11H7 was detected via real-time quantitative PCR (RT-qPCR) experiments. Specific bands for OR51E1 (~250 bp) and OR11H7 (~260 bp) were visible in agarose gels after amplification (A). Quantification of ΔCt values revealed a higher transcript abundance of OR51E1 (N = 3). (C) Transcript abundance of GNAL ($G\alpha_{olf}$) and ADCY3 (ACIII) was demonstrated via quantitative PCR. Specific bands for GNAL (~250 bp) and ADCY3 (~250 bp) were visible in agarose gels. (D, E, F) OR51E1, $G\alpha_{olf}$, and ACIII were expressed at the protein level. In western blot experiments, specific bands for OR51E1 (35 kDa), $G\alpha_{olf}$ (45 kDa) and ACIII (170 kDa) were detected. Immunocytochemical staining of HK-2 cells with specific antibodies for ACIII and $G\alpha_{olf}$ olfactory signaling components (G-H). (G, I) Specific staining (green) of ACIII in HK-2 cells validated its presence at the protein level. Detailed images of positively stained cells are shown on the right. (H, J) Specific staining (green) of $G\alpha_{olf}$ was observed in HK-2 cells. Cell nuclei were stained with DAPI. Scale bars: 20 μm. (For interpretation of the references to colour in this figure legend, the reader is referred to the web version of this article.)

OR51E1, $G\alpha_{olf}$, and ACIII also at the protein level in western blot experiments with specific antibodies (Fig. 2D, E, F). Because there are no specific antibodies for OR11H7, we could not verify the protein expression of OR11H7 in HK-2 cells. In immunocytochemical staining of HK-2 cells, specific staining of ACIII and $G\alpha_{olf}$ was detected in a subset of HK-2 cells (Fig. 2G–J).

3.3. Isovaleric acid-induced intracellular Ca^{2+} increase is dependent on the presence of extracellular Ca^{2+} and mediated by adenylyl cyclase III

IVA induced the strongest increase in intracellular Ca^{2+} concentration in HK-2 cells (see Fig. 1E). Therefore, we further investigated the underlying pathway downstream of OR51E1 activation using IVA as ligand. First, we determined the source of the calcium involved in the activation of the cells. Measurements under Ca^{2+}-free conditions (5 mM EGTA in the extracellular solution and no Ca^{2+}) revealed that the IVA (300 μM)-induced responses depend on extracellular Ca^{2+} (Fig. 3A). A highly significant reduction of the IVA-induced Ca^{2+} increase was observed in the absence of extracellular Ca^{2+} (amplitude: 0.0676 ± 0.0349) compared to the presence of extracellular Ca^{2+} (amplitude: 0.3958 ± 0.0757) (Fig. 3B). We then analyzed the effect of the adenylyl cyclase-specific inhibitor SQ22536 (200 μM) to demonstrate the involvement of ACIII in the signaling pathway. First, IVA was added to HK-2 cells and the intracellular Ca^{2+} increase was measured in Ca^{2+} imaging experiments. Then, cells were incubated with SQ22536 (200 μM) for 3 min after which IVA (300 μM) was added again in the presence of SQ22536 (Fig. 3C). The IVA-mediated Ca^{2+} response (amplitude: 0.5506 ± 0.1101) was completely abolished (amplitude: -0.0011 ± 0.0142) (Fig. 3D).

ACIII is co-localized with OR51E1 and $G\alpha_{olf}$ and the number of primary cilia correlates with cells responding to isovaleric acid.

In immunocytochemical staining of HK-2 cells after co-incubation with ACIII- and OR51E1-specific antibodies, we detected co-localization of these proteins in approximately 10% of all cells (Fig. 4A). Similarly, ACIII and $G\alpha_{olf}$ were also co-localized (Fig. 4B). Negative controls of anti-rabbit secondary antibodies co-incubated with anti-goat secondary antibodies showed no specific staining in both configurations (Suppl. Fig. 1). To analyze the presence of a primary cilium, HK-2 cells were stained with acetylated α-tubulin-specific antibody and visible primary cilia were counted (Fig. 4C and D). We demonstrated that 14.5561% ± 2.7955% of the cells form a primary cilium under the conditions tested (Fig. 4D). The number of cells forming a primary cilium (14.5561% ± 2.7955%) correlated with the number of cells responding to IVA in Ca^{2+} imaging experiments (10.2418% ± 1.3856%) (Fig. 4D).

3.4. OR51E1 is expressed at the protein level in human normal kidney tissue

To identify expression of OR51E1 at the protein level, we incubated paraffin-embedded kidney slices of two different human donors with OR51E1-specific antibodies and performed DAB-based

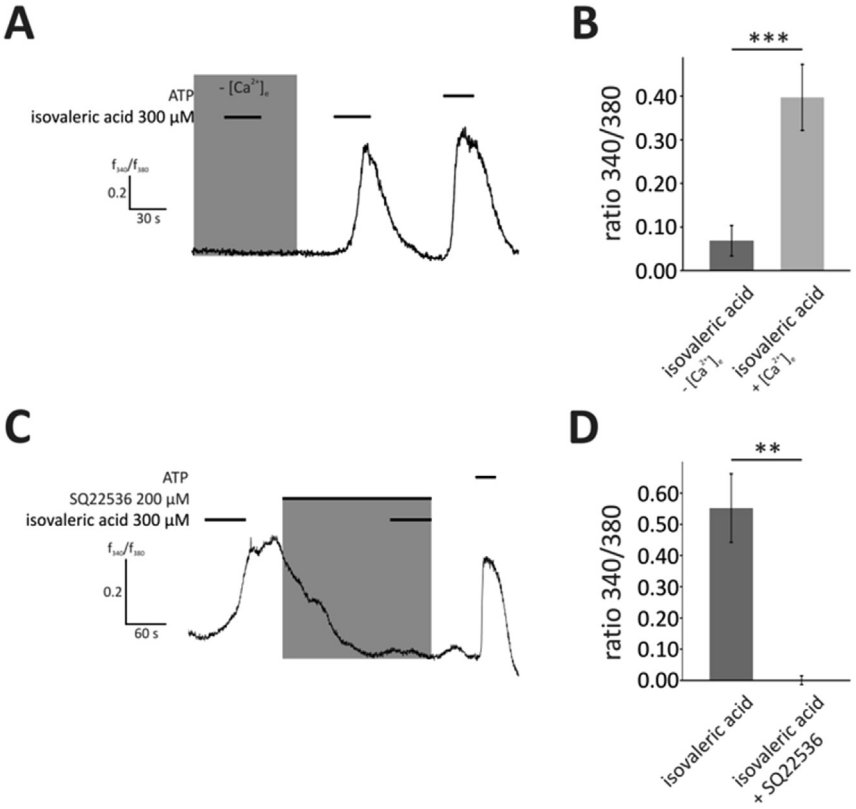

Fig. 3. Characterization of the isovaleric acid (IVA)-induced signaling pathway in HK-2 cells. (A, B) Intracellular Ca^{2+} increase in HK-2 cells upon application of IVA (300 μM) was dependent on the extracellular Ca^{2+} concentration. IVA (300 μM) was administered in Ca^{2+}-free solution containing 1 mM EGTA for 30 s. The Ca^{2+}-free solution was exchanged with normal Ringer's solution and IVA was reapplied for 30 s. IVA-induced amplitudes were quantified in the presence or absence of extracellular Ca^{2+} (B). A significant decrease in amplitude was observed in the absence of extracellular Ca^{2+} (N = 5). (C, D) Dependency of IVA-induced Ca^{2+} increase on adenylyl cyclase activation. SQ22536 (200 μM), a specific adenylyl cyclase inhibitor, was pre-incubated for 3 min and subsequently co-applied with IVA (300 μM) for 1 min (C). Quantification of the amplitudes revealed a significant inhibition of IVA (300 μM)-induced Ca^{2+} increase in the presence of SQ22536 (200 μM) (N = 4) (D). Black bars of all experiments indicate the stimulus duration. Gray bars indicate the application of either Ca^{2+}-free solution or SQ22536. As a viability control, ATP (100 μM) was added at the end of every measurement. All error bars represent the ±SEM of four or five independent experiments. Significance was tested using an unpaired two-sample Student's *t*-test. **p < 0.01; ***p < 0.001.

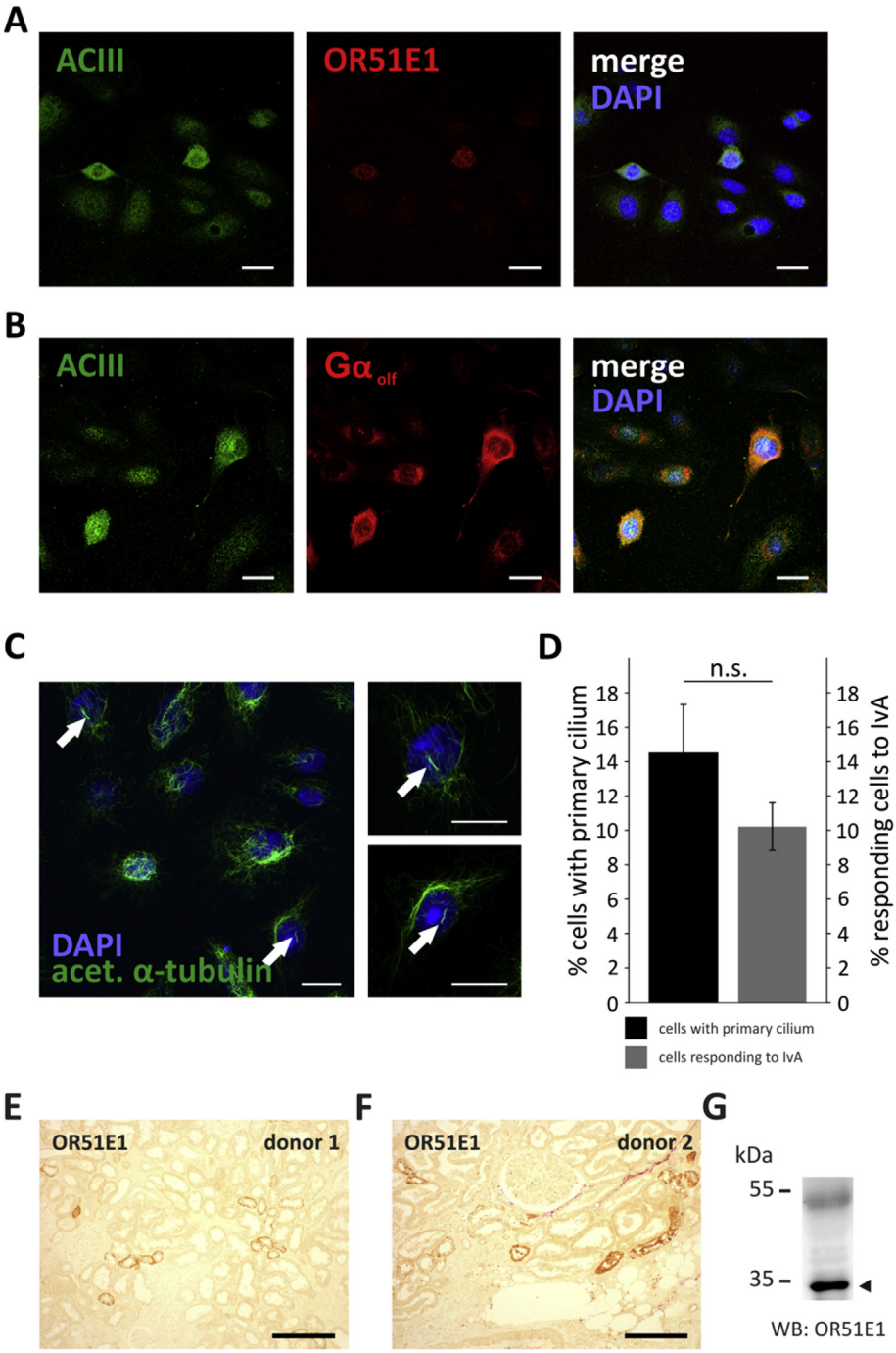

Fig. 4. Co-immunocytochemical staining of olfactory signaling components and correlation of OR51E1 with primary cilia in HK-2 cells (A–D). (A) Co-immunocytochemical staining of HK-2 cells revealed co-localization of ACIII and OR51E1. (B) Co-immunocytochemical staining showed co-localization of $G\alpha_{olf}$ and OR51E1. (C) Staining of HK-2 cells with acetylated α-tubulin. Arrows indicate visible primary cilia on the surface of HK-2 cells. (D) Quantification of cells with primary cilia and cells responding to isovaleric acid (IVA) in Ca^{2+} imaging experiments. All error bars represent the ±SEM of four or five independent experiments. Significance was tested using an unpaired two-sample Student's *t*-test. n.s.: $p > 0.05$. Scale bars: 20 μm OR51E1 protein was present in normal kidney tissue (E–G). (E, F) 3,3′-diaminobenzidine (DAB) staining of human kidney tissue from two different donors with an OR51E1-specific antibody. Staining was detected in parts of the tubule system of the nephron. A strong basal staining was detected in the tubule epithelia cells. (G) Western blot analysis of normal human kidney tissue protein lysate with OR51E1-specific antibody. A specific band of OR51E1 was visible at 35 kDa. Scale bars: 200 μm.

immunohistochemical staining (Fig. 4E and F). A strong and clear staining of parts of the tubules was detected in both donors. Interestingly, the basal part of the epithelia showed a stronger staining in several tubules. Western blot experiments with human kidney protein lysate revealed a specific band for OR51E1 at a height of 35 kDa (Fig. 4G).

4. Discussion

In this study, we demonstrated the activation of HK-2 cells by an odorant mixture containing three different fatty acids; two of which, IVA and 4-MVA, led to Ca^{2+} responses when applied to HK-2 cells. IVA and 4-MVA are both known agonists for human OR51E1 [18,21]. In general, OR51E1 seems to play a crucial role in sensing

fatty acids. In addition to the aforementioned ligands, nonanoic acid, 3-methylvaleric acid, and butyric acid are also described as agonists for heterogeneously expressed OR51E1 [18,22,23]. The expression of the pig orthologue to human OR51E1 has already been described in cells of the gastrointestinal tract and is believed to be involved in detecting bacterial metabolites [24]. IVA can also activate the receptors OR11H4, OR11H6, and OR11H7. OR11H7 expression is considered an important sensor for the detection of the "sweaty feet" odor [20]. Additionally, IVA is a metabolite of the leucine metabolism, and pathogenesis can lead to the autosomal recessive disorder isovaleric acidemia, which causes an increased concentration of IVA in the urine [15].

We verified the expression of OR51E1 and OR11H7 in HK-2 cells at the transcript level by quantitative PCR experiments. OR11H7 presents as an intact form and a non-functional form. Non-functional OR11H7 results from a nonsense mutation caused by a single nucleotide polymorphism (SNP) at the nucleotide position 679 that leads to a stop codon and a short defect [20].

The superfamily of ORs has approximately 350 functionally expressed members in humans; however, antibodies are available for just a few ORs. For the detection of OR51E1 at the protein level, we used an anti-OR51E1 antibody whose specificity was described elsewhere [16]. There are no known antibodies for OR11H7. Furthermore, we detected transcript abundance of the olfactory signaling components $G\alpha_{olf}$ and ACIII and validated their presence at the protein level via western blot experiments and immunohistochemical staining using specific antibodies. We observed that $G\alpha_{olf}$ and ACIII are co-expressed in HK-2 cells. This indicates that these essential proteins of the olfactory cAMP-mediated signaling pathway are present and could be involved in odorant-induced cytosolic Ca^{2+} increase. It was demonstrated that activation of ectopically expressed ORs can either lead to an intracellular Ca^{2+} increase through the cAMP-mediated pathway [3,5,6] or alternative signaling pathways such as phosphorylation of Src kinases and subsequent opening of TRP channels [25]. In our Ca^{2+} imaging experiments, IVA induced a strong and robust concentration-dependent Ca^{2+} increase; therefore, we further analyzed the pathway mediated by IVA. In the absence of extracellular Ca^{2+}, the response to IVA was completely abolished. Thus, we excluded Ca^{2+} release from intracellular stores as the source of the increase in cytosolic Ca^{2+} concentration. Inhibition of the Ca^{2+} increase was observed in the presence of the adenylyl cyclase blocker SQ22536. We therefore postulate that a cAMP-mediated signaling pathway is activated upon the application of IVA. In olfactory sensory neurons, the desensitization and inactivation of CNG channels and the phosphodiesterase-dependent degradation of cAMP leads to a rapid termination and transient Ca^{2+} elevation [26,27]. The transient Ca^{2+} elevation which is terminated during the application stimulus of OM, IVA, and 4-MVA (see Fig. 1A–C) leads to the conclusion that the underlying signaling pathway is similar to OR-signaling in the olfactory epithelium. Furthermore, this effect was observed in a small subset of cells. We therefore conclude that only a few cells express the functional OR-signaling repertoire. In the murine kidney, the classical olfactory signaling protein repertoire is also present [13]. In addition, the activation of the murine Olfr78 by short chain fatty acids modulates blood pressure, and the expression of murine ORs could be observed in the proximal tubule [14,28]. It has been shown, that the increase of intracellular Ca^{2+} in HK-2 cells is linked with various physiological processes. The activation of NMDA receptors and the subsequent influx of Ca^{2+} are critical for preserving the normal epithelial phenotype of proximal tubule cells [29]. Additionally, an increasing intracellular Ca^{2+} concentration can directly activate the Aurora A (AurA) kinase through calmodulin (CaM)-binding and is linked to polycystic kidney disease (PKD) [30,31]. Therefore, we suggest that Ca^{2+} influx mediated by the activation of OR51E1 can modulate the epithelial phenotype of HK-2 cells and might influence PKD. OR51E1 in human kidney tissue might also be involved in sensing fatty acids in the tubular fluid. Thus, we can speculate that OR51E1 has an impact on the regulation of blood pressure *in vivo*. However, these hypotheses need to be evaluated in further studies.

In previous studies, it was shown that HK-2 cells form primary cilia [32–34]. Under normal culture conditions, 10–30% of all cells are ciliated [35]. We showed that the presence of primary cilia in HK-2 cells correlates with the percentage of IVA-responding cells but could not observe a localization of OR51E1 in the cilia of the cells. Non-motile primary cilia can act as chemical and mechanical sensors, and their growth depends on the cell cycle [35,36]. Furthermore, vasopressin receptors mediate functional cAMP-signaling in primary cilia of renal epithelial cells [37]. In general, the polycystic proteins PKD1L1 and PKD2L1 form a heteromeric Ca^{2+} channel in primary cilia [38]. We suggest that the sensing of chemical stimuli in renal tubule cells should be investigated in more detail.

Taken together, this study provides new insights into the presence of ORs, which are commonly known as sensory receptors for fatty acids, in the human kidney. These findings could support the understanding of renal physiological and pathophysiological processes, such as PKD.

Funding

This research project was supported financially by the Deutsche Forschungsgemeinschaft (grant numbers SFB 874 and SFB 642) and the Ruhr-University Research School.

Acknowledgments

We thank Dr. Günter Gisselmann for his support regarding molecular biological techniques and Dr. Markus Heiland (Augusta-Krankenanstalten Bochum) for providing human biopsies. Furthermore, we thank Franziska Mößler, Andrea Stoeck and Petra Jergolla for their technical support.

Appendix A. Supplementary data

Supplementary data related to this article can be found at http://dx.doi.org/10.1016/j.abb.2016.09.017.

References

[1] L. Buck, R. Axel, A novel multigene family may encode odorant receptors: a molecular basis for odor recognition, Cell.. 65 (1991) 175–187, http://dx.doi.org/10.1016/0092-8674(91)90418-X.
[2] M. Spehr, G. Gisselmann, A. Poplawski, J.A. Riffell, C.H. Wetzel, R.K. Zimmer, H. Hatt, Identification of a testicular odorant receptor mediating human sperm chemotaxis, Science 80 (2003) 2054–2058, http://dx.doi.org/10.1126/science.1080376, 299.
[3] D. Maßberg, A. Simon, D. Häussinger, V. Keitel, G. Gisselmann, H. Conrad, H. Hatt, Monoterpene (-)-citronellal affects hepatocarcinoma cell signaling via an olfactory receptor, Arch. Biochem. Biophys. 566 (2015) 100–109, http://dx.doi.org/10.1016/j.abb.2014.12.004.
[4] E.M. Neuhaus, W. Zhang, L. Gelis, Y. Deng, J. Noldus, H. Hatt, Activation of an olfactory receptor inhibits proliferation of prostate Cancer cells, J. Biol. Chem. 284 (2009) 16218–16225, http://dx.doi.org/10.1074/jbc.M109.012096.
[5] S. Manteniotis, S. Wojcik, P. Brauhoff, M. Möllmann, L. Petersen, J. Göthert, W. Schmiegel, U. Dührsen, G. Gisselmann, H. Hatt, Functional characterization of the ectopically expressed olfactory receptor 2AT4 in human myelogenous leukemia, Cell. Death Discov. 2 (2016) 15070, http://dx.doi.org/10.1038/cddiscovery.2015.70.
[6] D. Busse, P. Kudella, N.-M. Grüning, G. Gisselmann, S. Ständer, T. Luger, F. Jacobsen, L. Steinsträßer, R. Paus, P. Gkogkolou, M. Böhm, H. Hatt, H. Benecke, A synthetic sandalwood odorant induces wound-healing processes in human keratinocytes via the olfactory receptor OR2AT4, J. Investig.. Dermatol. 134 (2014) 2823–2832, http://dx.doi.org/10.1038/jid.2014.273.

[7] T. Braun, P. Voland, L. Kunz, C. Prinz, M. Gratzl, Enterochromaffin cells of the human gut: sensors for spices and odorants, Gastroenterology 132 (2007) 1890–1901, http://dx.doi.org/10.1053/j.gastro.2007.02.036.
[8] H.A. Bakalyar, R.R. Reed, Identification of a specialized adenylyl cyclase that may mediate odorant detection, Science 250 (1990) 1403–1406. http://www.ncbi.nlm.nih.gov/pubmed/2255909.
[9] D.T. Jones, R.R. Reed, Golf: an olfactory neuron specific-G protein involved in odorant signal transduction, Science 244 (1989) 790–795. http://www.ncbi.nlm.nih.gov/pubmed/2499043.
[10] L. Belluscio, G.H. Gold, A. Nemes, R. Axel, Mice deficient in G(olf) are anosmic, Neuron 20 (1998) 69–81.
[11] J. Bradley, W. Bönigk, K. Yau, S. Frings, Calmodulin permanently associates with rat olfactory CNG channels under native conditions, Nat. Neurosci. 7 (2004) 705–710, http://dx.doi.org/10.1038/nn1266.
[12] R. Dhallan, K. Yau, K. Schrader, R.R. Reed, Primary structure and functional expression of a cyclic nucleotide-activated channel from olfactory neurons, Nature 347 (1990) 184–187.
[13] J.L. Pluznick, D.-J. Zou, X. Zhang, Q. Yan, D.J. Rodriguez-Gil, C. Eisner, E. Wells, C.A. greer, T. Wang, S. Firestein, J. Schnermann, M.J. Caplan, Functional expression of the olfactory signaling system in the kidney, Proc. Natl. Acad. Sci. U. S. A. 106 (2009) 2059–2064, http://dx.doi.org/10.1073/pnas.0812859106.
[14] J.L. Pluznick, R.J. Protzko, H. Gevorgyan, Z. Peterlin, A. Sipos, J. Han, I. Brunet, L.-X. Wan, F. Rey, T. Wang, S.J. Firestein, M. Yanagisawa, J.I. Gordon, A. Eichmann, J. Peti-Peterdi, M.J. Caplan, Olfactory receptor responding to gut microbiota- derived signals plays a role in renin secretion and blood pressure regulation, Proc. Natl. Acad. Sci. 110 (2013) 4410–4415, http://dx.doi.org/10.1073/pnas.1215927110.
[15] J. Vockley, R. Ensenauer, Isovaleric acidemia: new aspects of genetic and phenotypic heterogeneity, Am. J. Med. Genet. C. Semin. Med. Genet. 142C (2006) 95–103, http://dx.doi.org/10.1002/ajmg.c.30089.
[16] C. Flegel, F. Vogel, A. Hofreuter, B.S.P. Schreiner, S. Osthold, S. Veitinger, C. Becker, N.H. Brockmeyer, M. Muschol, G. Wennemuth, J. Altmüller, H. Hatt, G. Gisselmann, Characterization of the olfactory receptors expressed in human spermatozoa, Front. Mol. Biosci. 2 (2016), http://dx.doi.org/10.3389/fmolb.2015.00073.
[17] J.D. Mainland, A. Keller, Y.R. Li, T. Zhou, C. Trimmer, L.L. Snyder, A.H. Moberly, K.A. Adipietro, W.L.L. Liu, H. Zhuang, S. Zhan, S.S. Lee, A. Lin, H. Matsunami, The missense of smell: functional variability in the human odorant receptor repertoire, Nat. Publ. Gr 17 (2013) 114–120, http://dx.doi.org/10.1038/nn.3598.
[18] Y. Fujita, T. Takahashi, A. Suzuki, K. Kawashima, F. Nara, R. Koishi, Deorphanization of Dresden G protein-coupled receptor for an odorant receptor, J. Recept. Signal Transduct. Res. 27 (2007) 323–334, http://dx.doi.org/10.1080/10799890701534180.
[19] K. Audouze, A. Tromelin, A.M. Le Bon, C. Belloir, R.K. Petersen, K. Kristiansen, S. Brunak, O. Taboureau, Identification of odorant-receptor interactions by global mapping of the human odorome, PLoS One 9 (2014), http://dx.doi.org/10.1371/journal.pone.0093037.
[20] I. Menashe, T. Abaffy, Y. Hasin, S. Goshen, V. Yahalom, C.W. Luetje, D. Lancet, Genetic elucidation of human hyperosmia to isovaleric acid, PLoS Biol. 5 (2007) 2462–2468, http://dx.doi.org/10.1371/journal.pbio.0050284.
[21] J.D. Mainland, Y.R. Li, T. Zhou, W.L.L. Liu, H. Matsunami, Human olfactory receptor responses to odorants, Sci. Data 2 (2015) 150002, http://dx.doi.org/10.1038/sdata.2015.2.
[22] Y.R. Li, H. Matsunami, S. Materials, H. Press, B. This, S. Signaling, N.Y. Avenue, Activation state of the M3 muscarinic acetylcholine receptor modulates mammalian odorant receptor signaling, Sci. Signal 4 (2011), http://dx.doi.org/10.1126/scisignal.2001230 ra1.
[23] K.A. Adipietro, J.D. Mainland, H. Matsunami, Functional evolution of mammalian odorant receptors, PLoS Genet. 8 (2012) e1002821, http://dx.doi.org/10.1371/journal.pgen.1002821.
[24] D. Priori, M. Colombo, P. Clavenzani, A.J.M. Jansman, J.-P. Lallès, P. Trevisi, P. Bosi, The olfactory receptor OR51E1 is present along the gastrointestinal tract of pigs, Co-Localizes with enteroendocrine cells and is modulated by intestinal microbiota, PLoS One 10 (2015) e0129501, http://dx.doi.org/10.1371/journal.pone.0129501.
[25] J. Spehr, L. Gelis, M. Osterloh, S. Oberland, H. Hatt, M. Spehr, E.M. Neuhaus, G protein-coupled receptor signaling via Src kinase induces endogenous human transient receptor potential vanilloid type 6 (TRPV6) channel activation, J. Biol. Chem. 286 (2011) 13184–13192, http://dx.doi.org/10.1074/jbc.M110.183525.
[26] T. Leinders-Zufall, C.A. Greer, G.M. Shepherd, F. Zufall, Imaging odor-induced calcium transients in single olfactory cilia: specificity of activation and role in transduction, J. Neurosci. 18 (1998) 5630–5639.
[27] K.D. Cygnar, H. Zhao, Phosphodiesterase 1C is dispensable for rapid response termination of olfactory sensory neurons, Nat. Neurosci. 12 (2009) 454–462, http://dx.doi.org/10.1038/nn.2289.
[28] P. Rajkumar, W.H. Aisenberg, O.W. Acres, R.J. Protzko, J.L. Pluznick, Identification and characterization of novel renal sensory receptors, PLoS One 9 (2014), http://dx.doi.org/10.1371/journal.pone.0111053.
[29] M. Bozic, J. de Rooij, E. Parisi, M.R. Ortega, E. Fernandez, J.M. Valdivielso, Glutamatergic signaling maintains the epithelial phenotype of proximal tubular cells, J. Am. Soc. Nephrol. 22 (2011) 1099–1111, http://dx.doi.org/10.1681/ASN.2010070701.
[30] O.V. Plotnikova, E.N. Pugacheva, E.A. Golemis, Aurora A kinase activity influences calcium signaling in kidney cells, J. Cell. Biol. 193 (2011) 1021–1032, http://dx.doi.org/10.1083/jcb.201012061.
[31] O.V. Plotnikova, E.N. Pugacheva, R.L. Dunbrack, E.A. Golemis, Rapid calcium-dependent activation of Aurora-A kinase, Nat. Commun. 1 (2010) 1–8, http://dx.doi.org/10.1038/ncomms1061.
[32] E. van Rooijen, R.H. Giles, E.E. Voest, C. van Rooijen, S. Schulte-Merker, F.J. van Eeden, LRRC50, a conserved ciliary protein implicated in polycystic kidney disease, J. Am. Soc. Nephrol. 19 (2008) 1128–1138, http://dx.doi.org/10.1681/ASN.2007080917.
[33] S. Wang, Q. Wei, G. Dong, Z. Dong, ERK-mediated suppression of cilia in cisplatin-induced tubular cell apoptosis and acute kidney injury, Biochim. Biophys. Acta Mol. Basis Dis. 1832 (2013) 1582–1590, http://dx.doi.org/10.1016/j.bbadis.2013.05.023.
[34] T.R. Hartman, D. Liu, J.T. Zilfou, V. Robb, T. Morrison, T. Watnick, E.P. Henske, The tuberous sclerosis proteins regulate formation of the primary cilium via a rapamycin-insensitive and polycystin 1-independent pathway, Hum. Mol. Genet. 18 (2009) 151–163, http://dx.doi.org/10.1093/hmg/ddn325.
[35] O.V. Plotnikova, E.N. Pugacheva, E.A. Golemis, Primary cilia and the cell cycle, Methods Cell. Biol. 94 (2009) 137–160, http://dx.doi.org/10.1016/S0091-679X(08)94007-3.Primary.
[36] M. Delling, P.G. DeCaen, J.F. Doerner, S. Febvay, D.E. Clapham, Primary cilia are specialized calcium signalling organelles, Nature 504 (2013) 311–314, http://dx.doi.org/10.1038/nature12833.
[37] M.K. Raychowdhury, A.J. Ramos, P. Zhang, M. McLaughin, X.-Q. Dai, X.-Z. Chen, N. Montalbetti, M. Del Rocío Cantero, D.A. Ausiello, H.F. Cantiello, Vasopressin receptor-mediated functional signaling pathway in primary cilia of renal epithelial cells, Am. J. Physiol. Ren. Physiol. 296 (2009) F87–F97, http://dx.doi.org/10.1152/ajprenal.90509.2008.
[38] P.G. Decaen, M. Delling, T.N. Vien, D.E. Clapham, Direct recording and molecular identification of the calcium channel of primary cilia, Nature 504 (2013) 315–318, http://dx.doi.org/10.1038/nature13631.